



AB2-type amphiphilic block copolymer containing a pH-cleavable hydrazone linkage for targeted antibiotic delivery

Sandeep J. Sonawane^a, Rahul S. Kalhapure^{a,b,*}, Mahantesh Jadhav^a, Sanjeev Rambharose^{a,c}, Chunderika Mocktar^a, Thirumala Govender^{a,*}

^a Discipline of Pharmaceutical Sciences, School of Health Sciences, University of KwaZulu-Natal, Private Bag X54001, Durban 4000, South Africa

^b Odin Pharmaceuticals, 300 Franklin Square Drive, Somerset, NJ 08873, USA

^c Division of Emergency Medicine, Department of Surgery, University of Cape Town, Cape Town, South Africa



ARTICLE INFO

Keywords:

Hydrazone linkage
Amphiphilic polymer
pH cleavable
Vancomycin
MRSA
Site-specific delivery

ABSTRACT

A novel AB2-type amphiphilic block copolymer [OA-C=N-NH-(PEG)₂] with hydrazone linkage was synthesized and explored for pH-triggered antibiotic delivery. Vancomycin (VCM) loaded micelles of the polymer [OA-C=N-NH-(PEG)₂-VCM] were spherical in shape with size, polydispersity index, zeta potential and entrapment efficiency of 130.33 ± 7.36 nm, 0.163 ± 0.009 , -4.33 ± 0.55 mV and $39.61 \pm 4.01\%$ respectively. The dilution stability study exhibited no significant change in the size distribution of OA-C=N-NH-(PEG)₂-VCM micelles up to 320-fold dilution. An *in vitro* drug release assay confirmed greater release of VCM from OA-C=N-NH-(PEG)₂-VCM at pH 6, compared to pH 7.4. An *in vitro* antibacterial activity evaluation of OA-C=N-NH-(PEG)₂-VCM showed 2-fold enhancement in antibacterial activity of VCM after 54 h of incubation against *Staphylococcus aureus* (*S. aureus*) and methicillin-resistant *S. aureus* (MRSA) at acidic pH compared to physiological pH. An *in vivo* antibacterial activity of OA-C=N-NH-(PEG)₂-VCM further proved the enhanced activity of OA-C=N-NH-(PEG)₂-VCM against MRSA. In conclusion, micelles from pH-responsive OA-C=N-NH-(PEG)₂ could be utilized for site-specific delivery of VCM at the infection site.

1. Introduction

Most bacterial species have developed clinically significant resistance towards available antibiotics due to frequent and suboptimal use of antibiotics in treating bacterial infections (Sharma et al., 2012). Misuse and overuse of antibiotics especially in developing countries have contributed to evolution of resistant bacteria such as methicillin-resistant *Staphylococcus aureus* (MRSA), vancomycin-resistant *Staphylococcus aureus* (VRSA) and vancomycin-resistant *Enterococcus* (VRE) (Fernandes and Martens, 2017; Klevens et al., 2006; Rice, 2009). The development of new antibiotics is in a stagnant phase and the available pool of antibiotics is not sufficient enough to address the risk of rapidly growing antibiotic resistance crisis (Allahverdiyev et al., 2011;

Fernandes and Martens, 2017; Sharma et al., 2012). Therefore, the design and development of novel strategies for efficient delivery of currently existing antibiotics to improve their efficacy so that they can combat bacterial resistance more effectively is necessary (Kalhapure et al., 2014).

Nanotechnology has proved to be an effective strategy to address the problems related to antibiotic resistance (Pelgrift and Friedman, 2013). Conventional dosage forms of antibiotics have various disadvantages including occurrence of bacterial resistance with time, non-targeted delivery to the infections site, low therapeutic index, undesired side effects and enhanced frequency of administration. These limitations can be overcome using various nanoparticulate drug delivery systems (Bawa et al., 2009; Sharma et al., 2012). Various

Abbreviations: MRSA, methicillin-resistant *Staphylococcus aureus*; VRSA, vancomycin-resistant *Staphylococcus aureus*; VRE, vancomycin-resistant *Enterococcus*; NEs, nanoemulsions; PNPs, polymeric nanoparticles; SLNs, solid lipid nanoparticles; LPHNs, lipid polymer hybrid nanoparticles; LDHNS, lipid dendrimer hybrid nanoparticles; MHA, Mueller Hinton Agar; MHB, Mueller-Hinton broth; MTT, 3-(4,5-Dimethylthiazol-2-yl)-2,5-diphenyltetrazolium bromide; FT-IR, Fourier-transform infrared; ¹H NMR, proton nuclear magnetic resonance; ¹³C NMR, carbon nuclear magnetic resonance; HRMS, high resolution mass spectrometry; RBF, round bottom flask; NIBS, non-invasive back scatter; LCMS, liquid chromatography-mass spectrometry; DCM, dichloromethane; VCM, vancomycin; TEM, transmission electron microscope; PI, polydispersity index; ZP, zeta potential; RT, room temperature; SD, standard deviation; CFU, colony forming units; ANOVA, analysis of variance; CMC, critical micelle concentration; TLC, thin layer chromatography; RF, retention factor; MIC, minimum inhibitory concentration

* Corresponding authors at: Private Bag X54001, Durban 4000, KwaZulu-Natal, South Africa.

E-mail addresses: kalhapure@ukzn.ac.za (R.S. Kalhapure), govenderth@ukzn.ac.za (T. Govender).

<https://doi.org/10.1016/j.ijpharm.2019.118948>

Received 1 August 2019; Received in revised form 1 December 2019; Accepted 7 December 2019

Available online 16 December 2019

0378-5173/ © 2019 Elsevier B.V. All rights reserved.

nanoparticulate drug delivery systems have been reported in the literature for efficient delivery of antibiotics. These nano systems include; nanoemulsions (NEs), polymeric nanoparticles (PNPs), solid lipid nanoparticles (SLNs), liposomes, dendrimers, lipid polymer hybrid nanoparticles (LPHNs), lipid dendrimer hybrid nanoparticles (LDHNs) (Sonawane et al., 2016), and nanostructures composed of pure carbon and nanohybrids (Kalhapure et al., 2015).

Although these nanoantibiotics are therapeutically effective compared to conventional dosage forms (Kalhapure et al., 2015), they are not smart enough to respond to the changes in metabolic states of the body (Bawa et al., 2009). Ideally, the release of a drug from a delivery system should be in accordance with the physiological need of the body (Gupta et al., 2002). Therefore, application of stimuli-responsive drug delivery systems using different triggers for drug targeting to the site of action has become a major focus area (Ganta et al., 2008; Kalhapure and Renukuntla, 2018). Amongst different stimuli, pH has been studied widely for site specific drug delivery (Liu et al., 2016). The materials employed for preparing pH-responsive drug delivery systems contain a particular chemical functional group in their structure that can show response to various pH gradients existing in both normal and disease conditions in the body (Gillies et al., 2004). Various chemical functional groups, such as, ortho ester (Tang et al., 2011; Tang et al., 2010), acetal (Chen et al., 2010; Kim et al., 2010), vinyl ether (Shin et al., 2003; Xu et al., 2008), amine (Lee et al., 2003; Radovic-Moreno et al., 2012) and hydrazone (Bae et al., 2003; Etrych et al., 2010) have been utilized to fabricate materials that are efficient to release their payload at the lower pH conditions, specifically in the management of various cancerous tumours. To date only three to four papers have reported use of pH-responsive materials for antibiotic delivery, including a pH-responsive surfactant (Kalhapure et al., 2017a) and lipids (Jadhav et al., 2018; Kalhapure et al., 2017b; Mhule et al., 2018).

The hydrazone linkages have been commonly used for conjugating drugs to polymer backbones to design pH-responsive delivery systems due to their rapid hydrolysis at acidic pH compared to neutral physiological pH, the purpose being to minimize systemic toxicity by targeting drug to the site of action in the body (Yoshida et al., 2013). Hydrazone linkages have been proven to be an effective strategy in designing several pH-responsive drug delivery systems, such as linear polymers (Lu et al., 2009), star shaped polymers (Etrych et al., 2011), dendrimers (Kono et al., 2008), micelles (Aryal et al., 2009) and PEGylated systems (Lai et al., 2010) for the site specific delivery of anticancer drugs. The site specific delivery of anticancer drugs reported in most of the articles has been achieved through hydrazone conjugates formed by conjugating hydrazide functional group of carrier polymers or inorganic materials or dendrimers with an aldehyde or ketone functional group of anticancer drugs (Sonawane et al., 2017). Although the hydrazone conjugates have been reported to be effective systems for the site specific delivery of anticancer drugs, their limitations must be taken into consideration for design of new pH-responsive systems for other classes of drugs containing no ketone or aldehyde functional group in their structures. In the present available pool of various drug classes, very few contain aldehyde or ketone functional groups in their structures. For example, only doxorubicin and pirarubicin from the anticancer class and streptomycin antibiotic fulfill the criterion of possessing aldehyde/ketone function in their structures for the formation of pH-responsive hydrazone bond with hydrazide functional group of various carriers (Sonawane et al., 2017). Considering the limitations associated with hydrazone conjugates and since there are very few reports on a polymer itself containing hydrazone linkage, there is an urgent need to design and develop a novel polymer containing hydrazone linkage for encapsulation and site specific delivery of any class of drugs. An inadequate concentration of antibiotics at the bacterial infection site is one of the reasons for the evolution of resistant bacterial species by supporting gene mutations (Kalhapure et al., 2017b). Design and development of novel responsive materials for site specific antibiotic delivery to maximize its utilization and reduce elimination via

systemic circulation will certainly solve the problem of superbugs by improving antibiotic efficiency. Among various responsive materials, use of pH-responsive materials could be an effective approach for delivery of sufficient amount of antibiotics specifically at infection site, as bacterial infection sites are known for acidic conditions (Kalhapure et al., 2017b; Radovic-Moreno et al., 2012). Various researchers have shown promise of developing new polymers with pH-responsiveness to antibiotic delivery. However, the reported polymers require difficult synthesis and purification steps, the use of hazardous chemicals for their synthesis and purification, and have low production yields.

Thus, a new AB₂ type amphiphilic block copolymer containing a pH-cleavable hydrazone linkage was designed, synthesized by conjugation of aldehyde functional group of PEG aldehyde with carbonylhydrazide function of G1 oleodendrimer (Kalhapure and Akamanchi, 2013), and utilized for pH-responsive delivery of vancomycin (VCM). This polymer was successfully used in the formulation development of VCM loaded polymeric micelles, which showed pH-dependent enhanced drug release and antibiotic activity against both susceptible and resistant *S. aureus* strains.

The goal of the research undertaken in this manuscript was primarily to enhance antibacterial potency of VCM against susceptible and resistant bacteria through a pH-responsive micellar delivery system to specifically target the infection site. The promising *in vitro* and *in vivo* results obtained through this study are presented in this manuscript.

2. Materials and methods

2.1. Materials

Benzyl amine, methyl acrylate, thionyl chloride and trimethylamine were purchased from Merck Chemicals (Germany). Pd/C (10%), oleic acid, hydrazine hydrate solution (50–60%) and poly (ethylene glycol) methyl ether (average Mn = 5000) were procured from Sigma-Aldrich Co., Ltd. (USA). All the solvents utilized were of analytical grade and procured from Merck Chemicals (Germany). VCM was obtained from Sinobright Import and Export Co., Ltd. (China). Nutrient Broth and Mueller Hinton Agar (MHA) were procured from Biolab Inc., (South Africa). Mueller-Hinton broth (MHB) was obtained from Oxoid Ltd. (England), and 3-(4,5-Dimethylthiazol-2-yl)-2,5-diphenyltetrazolium bromide (MTT) from Merck Chemicals (Germany). All other chemicals used in this research work were obtained from Sigma-Aldrich Co., Ltd. (USA). Distilled water used was obtained in the laboratory with a Milli-Q purification system (Millipore corp., USA). For antibacterial studies, *S. aureus* (ATCC 25922) and *S. aureus* Rosenbach (ATCC®BAA-1683TM) (MRSA) were used. Fourier-transform infrared (FT-IR) spectra of all the synthesized molecules were produced on a Bruker Alpha-p spectrometer with diamond ATR (Germany), as per standard procedures. Proton and carbon nuclear magnetic resonance (¹H NMR and ¹³C NMR) spectra were determined using a Bruker 400/600 Ultrashield™ (U.K.) NMR spectrometer. High resolution mass spectrometry (HRMS) spectra were obtained on a Waters Micromass LCT Premier TOF-MS (U.K.).

2.2. Methods

2.2.1. Synthesis of OA-C=N-NH-(PEG)₂ (Fig. 1)

2.2.1.1. Synthesis of compounds (i) to (iv). A procedure reported in the previous literature was followed for the synthesis of compounds (i) to (iv) (Kalhapure and Akamanchi, 2013).

2.2.1.2. Synthesis of compound (v). Compound (iv) (0.5 g, 1.102 mmol) in ethanol (20 ml) was added drop wise to an ethanolic solution (30 ml) of hydrazine hydrate (50–60%) (quantity equivalent to approx. 1.41 g, 44.08 mmol of pure hydrazine) in 100 ml of round bottom flask (RBF) over a period of 30 min. After complete addition of hydrazine hydrate, the resulting mixture was heated under reflux for 12 h. The ethanol and residual amount of hydrazine hydrate were removed, using a rotary

evaporator and the obtained product was further freeze dried to completely remove entrapped water from product. Complete removal of water yielded a light yellow semisolid (0.455 g, 91.07%).

2.2.1.3. Synthesis of mPEG-aldehyde (mPEG-CHO). mPEG-CHO was synthesized from poly (ethylene glycol) methyl ether (average Mn = 5000) according to a previously reported method (Sugimoto et al., 1998).

2.2.1.4. Synthesis of compound (vi) [OA-C=N-NH-(PEG)₂]. Compound (v) (0.435 g, 0.958 mmol) and mPEG-CHO (12 g, 2.4 mmol) were dissolved in chloroform (200 ml) in 500 ml of RBF and heated under reflux for 24 h. The progress of reaction was monitored using FT-IR spectrophotometer. The product was purified by dialyzing against 500 ml of methanol for 48 h (fresh methanol was replaced after each 12 h for 2 days) using 7000 MWCO dialysis tubing (Thermo Scientific, U.S.A.), followed by removal of methanol using a rotary evaporator to get a light yellowish-white solid (4.5 g, 45%).

2.2.2. Characterization of compounds

Structural characterization of compound (v) and (vi) was performed using FT-IR spectroscopy (Bruker Alpha-p spectrometer with diamond ATR, Germany), ¹H NMR and ¹³C NMR spectroscopy (Bruker 400/600 Ultrashield™ NMR spectrometer, U.K.) and HRMS spectrometry on a Waters Micromass LCT Premier TOF-MS (U.K.).

2.2.3. Critical micelle concentration (CMC)

The CMC of the synthesized OA-C=N-NH-(PEG)₂ was determined according to a previously reported dynamic light scattering method (Topel et al., 2013). Zetasizer Nano ZS (Malvern Instruments Ltd., UK) was utilized to determine the scattered intensity from each solution of different concentration of OA-C=N-NH-(PEG)₂. The scattered intensity measurements were carried out at an angle of 175° in order to maintain the non-invasive back scatter (NIBS) optic arrangement, which increases the detection of scattered light while retaining signal quality. The solutions of different concentrations ranging from 1 to 30 µg/ml were prepared using stock solution (1 mg/ml) of OA-C=N-NH-(PEG)₂ in water. All the measurements were carried out in triplicate using a polystyrene cell at 25 °C.

2.2.4. pH dependent breakdown

In vitro hydrolytic breakdown of hydrazone linkage present in the OA-C=N-NH-(PEG)₂ was assessed by incubating 20 mg of polymer in 10 ml of PBS at pH 6 and 7.4 at 37 °C. After a period of 4, 8, 16 and 24 h of incubation, aliquots of polymeric solution in PBS were collected and analyzed using liquid chromatography-mass spectrometry (LCMS) analysis. LCMS analysis was performed using Shimadzu mass spectrometer (Japan) equipped with an Xbridge C18 (4.6 × 100 mm, 3.5 mm) column. The mobile phases prepared for analysis were 0.1% formic acid in acetonitrile (mobile phase A), and 0.1% formic acid in water (mobile phase B). A linear gradient, from 5 to 95% of B (water, 0.1% formic acid) into A (acetonitrile, 0.1% formic acid) at a flow rate of 1 ml/min, was used for the analysis.

2.2.5. In vitro cytotoxicity study

In vitro cytotoxicity of the OA-C=N-NH-(PEG)₂ against adenocarcinomic human alveolar basal epithelial cells (A549), breast cancer cell line (MCF7) and human liver hepatocellular carcinoma (HepG2) cell lines was tested using an MTT assay. A 96-well plate was employed to equivalently seed the cell lines (2.5 × 10³) and further allowed to adhere by incubating for 24 h. Following adherence, the fresh culture medium was placed in the wells and aqueous solutions of OA-C=N-NH-(PEG)₂ was added to attain final concentrations of 20–100 µg/ml. The controls were prepared by adding culture medium only, whilst wells with media only were used as blanks. The plates were further incubated (48 h), the wells were replenished with the fresh media (100 µl) and

5 mg/ml MTT solution in PBS (100 µl) and incubated for 4 h. Thereafter, MTT containing solution was discarded, and DMSO (100 µl) was introduced into the wells to solubilize the MTT formazan. Absorbance was measured at 540 nm wavelength. A microplate spectrophotometer (Mindray MR-96A) was used for this purpose (Sonawane et al., 2015). The equation used to calculate the percentage cell viability was as follows:

$$\% \text{ cell survival} = \frac{[\text{A540 nm treated cells}]}{[\text{A540 nm untreated cells}]} \times 100$$

2.2.6. Preparation of VCM loaded micelles [OA-C=N-NH-(PEG)₂-VCM]

OA-C=N-NH-(PEG)₂-VCM micelles were prepared using emulsification method. Briefly, 100 mg of OA-C=N-NH-(PEG)₂ was dissolved in 1 ml of dichloromethane (DCM) and added drop by drop through the sidewall of a beaker containing 10 mg of VCM dissolved into 10 ml of pH 7.4 PBS. The resulting emulsion was allowed to stir overnight for the complete removal of DCM. A similar method was followed to prepare VCM free (blank) micelles.

2.2.7. Determination of particle size, polydispersity index (PI) and zeta potential (ZP)

The measurement of particle size, PI and ZP of OA-C=N-NH-(PEG)₂-VCM was performed using the dynamic light scattering method after diluting OA-C=N-NH-(PEG)₂-VCM micelles solution (200 µl) with milli-Q water (1 ml). The PI value represented size distribution, and ZP value showed the total charge present on the surface of micelles (Sonawane et al., 2015).

2.2.8. Surface morphology

Surface morphology of OA-C=N-NH-(PEG)₂-VCM micelles was investigated using transmission electron microscope (TEM). A drop of suitably diluted micelles was allowed to dry on a copper grid (300 mesh) coated with a 3 mM forman (0.5% plastic powder in amyl acetate), and uranyl acetate stain (2% w/v) was further added for 30 sec, dried. A 100 kV of accelerating voltage was used to visualize micelles using a mega view III camera (Jeol, JEM-1010, Tokyo, Japan).

2.2.9. Entrapment efficiency (% EE) and drug loading capacity (LC)

The total amount of VCM entrapped in OA-C=N-NH-(PEG)₂-VCM micelles was determined using an ultrafiltration method (Sonawane et al., 2016). Briefly, 2 ml of micelle solution was filled into Amicon® Ultra-4 centrifugal filter tube (Millipore Corp., USA) having molecular weight cut-off of 10 kDa, and allowed to centrifuge at 300g at 25 °C for 30 min. The filtrate containing untrapped amount of VCM was analyzed using UV spectrophotometer (Schimadzu UV 1601, Japan) at 280.5 nm, with appropriate blanks. The regression equation and linearity (r²) obtained were y = 0.004x + 0.0082 and 0.9991, respectively. The method was specific, as blank micelles showed no interference at the specified wavelength. The following equations were used to calculate the % EE and LC of OA-C=N-NH-(PEG)₂-VCM micelles (Sonawane et al., 2016; Wang et al., 2012):

$$\% \text{ EE} = \left(\frac{\text{Weight of VCM in micelles}}{\text{Weight of VCM added}} \right) \times 100\%$$

$$\text{LC} = \left(\frac{\text{Weight of VCM in micelles}}{\text{Weight of micelles}} \right) \times 100\%$$

2.2.10. Dilution stability of the OA-C=N-NH-(PEG)₂-VCM micelles

The dilution stability of the OA-C=N-NH-(PEG)₂-VCM micelles was studied by slight modifications in previously reported method (Song et al., 2014). In brief, the micelles sample (containing 10 mg/ml of OA-C=N-NH-(PEG)₂) was diluted using PBS (pH 7.4) from 1.25 to 320-fold at room temperature (RT), and changes in particle size were determined using Zetasizer Nano ZS (Malvern Instruments Ltd., UK).

2.2.11. *In vitro* drug release

OA-C=N-NH-(PEG)₂-VCM micelles, blank micelles and bare VCM solution (1 ml) (donor solutions) were added in dialysis tubes (molecular weight: 8000–14,400 Da), and dialysis was performed against 40 ml of PBS at pH 6 and 7.4 (receiver solutions), respectively, in 50 ml bottles at 37 °C in an incubator at 100 rpm. At fixed time intervals, samples (3 ml) from the receiver solutions were withdrawn for analysis and replaced with an equal volume of fresh PBS (pH 6 and 7.4) to maintain sink conditions. The amount of VCM released after each time interval was determined spectrophotometrically at 280.5 nm and 280.4 nm at pH 7.4 and 6, respectively with blank micelles as a reference. The regression equation and linearity (r^2) obtained at pH 7.4 were $y = 0.004x + 0.0082$ and 0.9991, respectively, whereas at pH 6 they were $y = 0.0043x + 0.0004$ and 1, respectively. This experiment was performed in three replicates.

2.2.12. *In vitro* antibacterial activity

A broth dilution method was used to determine the minimum inhibitory concentration (MIC) values for bare VCM and OA-C=N-NH-(PEG)₂-VCM micelles against *S. aureus* and MRSA at 18, 36 and 54 h at pH 7.4 and 6, respectively. Briefly, a densitometer (DEN-1B densitometer, Shanghai, China) was used to adjust overnight grown cultures of *S. aureus* and MRSA to 0.5 McFarland, and subsequently diluted (1:150) using distilled water to obtain 1×10^6 CFU/ml. The serial dilutions of the test samples at pH 7.4 and 6 were performed by adding 135 μ l of bare VCM solution and OA-C=N-NH-(PEG)₂-VCM micelles to each well of a 96-well plate containing 135 μ l of MHB of pH 7.4 and 6, respectively. To the serially diluted samples, bacterial cultures (15 μ l) were added and further allowed to incubate in a shaking incubator at 37 °C, for 18 h at 100 rpm. The MIC values at pH 7.4 and 6 were determined by spotting the respective dilutions (5 μ l) on MHA plates and allowing to incubate for 18, 36 and 54 h. Blank micelles were used as the control. All the experiments were performed in three replicates.

2.2.13. *In vivo* antibacterial activity

The *in vivo* antibacterial activity of plain VCM and OA-C=N-NH-(PEG)₂-VCM micelles was performed against MRSA using BALB/c mice. The protocol (Protocol No. AREC/104/015PD) followed for this study was approved by Animal Research Ethics Committee (AREC) of the University of KwaZulu-Natal (UKZN). The guidelines developed by the AREC of UKZN and South African National Standard (SANS 10386:2008) were followed for the human care of the animals used in this study. A day prior to the experiments, male BALB/c mice ($n = 4$ for each group) were shaved to remove the back hairs, and the shaved skin was disinfected with ethanol. The following day, 50 μ l of 0.5 McFarland of MRSA suspension in sterile saline was injected intradermally at the shaved area at the back of all the animals. After 20 min, plain VCM and OA-C=N-NH-(PEG)₂-VCM micelles (50 μ l; equivalent to 25 μ g/ml of VCM) were injected at the same place as the MRSA infection. The mice were observed over 48 h for lesion development. Thereafter, the mice were then euthanized, and the infected skin was surgically removed and homogenized in sterile PBS (8 ml). The achieved suspensions were diluted 10^1 to 10^4 , and 20 μ l of each diluted sample was spotted on a nutrient agar plate and incubated overnight at 37 °C, to quantify the number of colony forming units (CFU) of MRSA in the skin tissues. The following equation was used to calculate the CFU/ml:

CFU/ml

$$= (\text{number of colonies} \times \text{dilution factor}) / \text{volume of culture plate}$$

Morphological evaluations were made on freshly harvested samples from the injection site. After harvesting, the skin was moved from saline to 10% buffered formalin. After 7 days, skin samples were embedded in paraffin wax following dehydration in an ethanol gradient. A microtome (Leica RM2235, Leica Biosystems, Germany) was used to section the tissue wax blocks. Sections were collected and dried on slides and

further allowed to stain with hematoxylin and eosin (H&E). A Leica Microscope DM 500, fitted with a Leica ICC50 HD camera (Leica Biosystems, Germany) was used to examine the sections and capture the images.

2.2.14. Stability studies

The physical stability assessment of OA-C=N-NH-(PEG)₂-VCM micelles was performed for three months both at room temperature and at 4 °C. Various parameters such as particle size, PI, ZP and appearance were considered for the physical stability assessment.

2.2.15. Statistical analysis

The data generated is stated as mean \pm standard deviation (SD), and bio-statistical analysis was performed using one-way analysis of variance (ANOVA), followed by non-parametric Kruskal-Wallis and paired *t*-test were used. GraphPad Prism (Graph Pad Software Inc., Version 5, San Diego, CA) software was used for statistical analysis and a *p* value < 0.05 was considered statistically significant.

3. Results and discussion

3.1. Synthesis and characterization of newly synthesized compound (v) and (vi)

Compound (v) containing hydrazide functional groups was synthesized by refluxing hydrazine hydrate with an ethanolic solution of compound (iv) containing ester functional groups. Then, OA-C=N-NH-(PEG)₂ (compound-vi) polymer containing hydrazone linkage was synthesized by conjugating m-PEG-CHO to the free hydrazide functional groups of the compound (v).

3.1.1. Compound (v)

Light yellow semi-solid, FT-IR: 3317.52, 3288.93, 2956.70, 2871.33, 1628.60, 1533.97, 1471.77, 1378.26, 1260.62, 1161.86 cm^{-1} . ¹H NMR (CDCl₃) δ (ppm): 0.81 (t; 3H; -CH₃), 1.19–1.23 (m; 20H; -CH₂-), 1.49 (q; 2H; -CH₂CH₂CON-), 1.94 (m; 4H; -CH₂CH=CHCH₂-), 2.29 (t; 2H; -CH₂CON-), 2.41 (t; 4H; -N(CH₂CH₂CONH-)₂), 3.45–3.57 (t; 4H; -N(CH₂CH₂CONH-)₂), 3.97 (bs; 4H; -NHNH₂), 5.26 (m; 2H; -CH=CH-). ¹³C NMR (CDCl₃) δ (ppm): 14.10, 22.67, 25.44, 27.24, 29.28–29.77, 31.90, 31.92, 33.22, 33.84, 43.35, 45.20, 129.69, 130.02, 170.85, 172.14, 174.52. ESI-TOF MS *m/z*: [M+Na]⁺ - calculated 476.3577 (C₂₄H₄₇N₅O₃+Na⁺), found 476.3581.

3.1.2. Compound (vi)

Light yellowish-white solid, melting point = 64 °C, FT-IR: 2881.23, 2739.36, 1683.11, 1642.22, 1466.24, 1358.74, 1340.52, 1279.25, 1145.79, 1101.86 cm^{-1} . ¹H NMR (CDCl₃) δ (ppm): 0.81 (t; 3H; -CH₃), 1.19–1.23 (m; 20H; -CH₂-), 1.52 (q; 2H; -CH₂CH₂CON-), 1.93 (m; 4H; -CH₂CH=CHCH₂-), 2.29 (t; 2H; -CH₂CON-), 2.41 (t; 4H; -N(CH₂CH₂CONH-)₂), 3.30 (s; 3H; -CH₃), 3.45–3.47 (t; 4H; -N(CH₂CH₂CONH-)₂), 3.57–3.69 [m; CH₂ of PEG (-OCH₂CH₂O- chain)], 4.14 (t; 4H; -N=CHCH₂-), 4.61 (t; 4H; -N=CHCH₂-), 5.26 (m; 2H; -CH=CH-), 8.02 (t; 1H; -N=CHCH₂-). ¹³C NMR (CDCl₃) δ (ppm): 13.81, 14.16, 20.94, 22.66, 27.22, 29.28–29.76, 31.88, 58.99, 61.61, 62.99, 63.41, 63.58, 66.29, 67.08–70.60, 71.97, 72.68, 74.92, 129.84, 160.99, 164.66, 170.87. ESI-TOF MS *m/z*: [M-10413.6700], [M+6/6] - calculated 1736.6116, found 1736.8472.

3.2. Critical micelle concentration (CMC)

The CMC of OA-C=N-NH-(PEG)₂ was determined at 25 °C, using dynamic light scattering method to determine micelle formation capability and stability of micelles for site specific delivery of the encapsulated drug. To obtain the CMC value of OA-C=N-NH-(PEG)₂ polymer, the intensity values of scattered light obtained from each

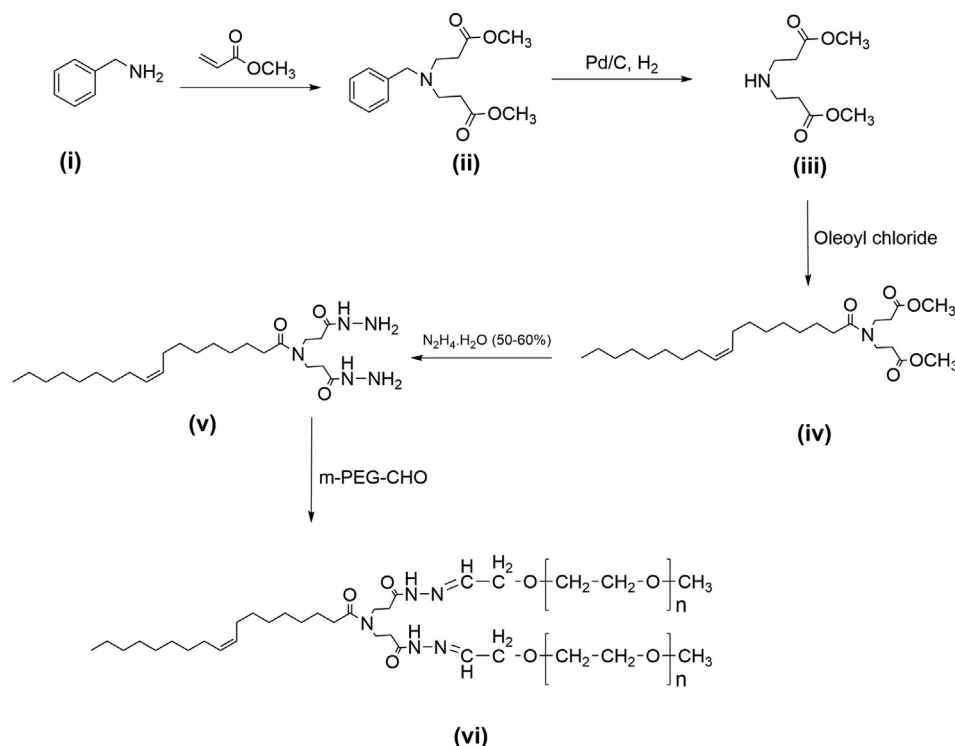


Fig. 1. Synthesis of AB₂ type amphiphilic block copolymer [OA-C=N-NH-(PEG)₂] containing hydrazone linkage.

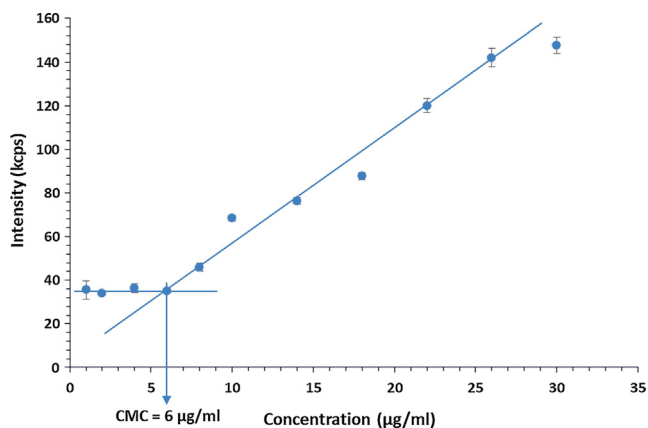


Fig. 2. Determination of the critical micelle concentration of OA-C=N-NH-(PEG)₂ polymer using dynamic light scattering measurements.

solution of different concentration of OA-C=N-NH-(PEG)₂ polymer were plotted against different concentrations of OA-C=N-NH-(PEG)₂ polymer. This plot of intensity versus concentration yielded two straight lines intersecting at data points corresponding to 6 µg/ml. This value indicates the CMC value of OA-C=N-NH-(PEG)₂ polymer (Fig. 2), which was found to be much lower compared to previously reported CMC value (0.87 mg/L) of tri-block copolymer (PEG-DiHyd-PLA-18K) containing hydrazone linkages (Qi et al., 2018).

The scattered intensity values obtained for OA-C=N-NH-(PEG)₂ concentrations below CMC were almost constant, corresponding to that of deionized water, as reported previously (Topel et al., 2013). Whereas, there was linear increase in the intensity with concentration at the CMC because of increase in number of micelles in the solution. The CMC values are important to decide the stability of micelles for *in vivo* applications. A low CMC provides stability to polymeric micelles by allowing great resistance to dilution (Sahoo and Labhassetwar, 2003; Song et al., 2014). Therefore, the low CMC (6 µg/ml) obtained in this study indicates that the micelle structure formed by OA-C=N-NH-

(PEG)₂ would remain stable even upon severe dilution in the bloodstream following intravenous injection. This further indicates the suitability of an amphiphilic polymer [OA-C=N-NH-(PEG)₂] as a drug carrier for *in vivo* applications.

3.3. pH dependent breakdown

Hydrolytic breakdown (degradation) of polymers is considered as an important step in achieving controlled and site specific delivery of drugs to the target sites (Liechty et al., 2010). Therefore pH dependent degradation behaviour of the newly synthesized polymeric assemblies containing hydrazone linkages at various physiological pH is essential. The degradation of OA-C=N-NH-(PEG)₂ polymer was performed in PBS at pH 6 and 7.4, respectively at 37 °C for 24 h. Initially, a thin layer chromatography (TLC) method was tried for monitoring progress of the degradation process, but similar retention factor (RF) values of degradation product (compound-v) and OA-C=N-NH-(PEG)₂ polymer (compound-vi) complicated the interpretation of results. Therefore, aliquots of polymeric solution in PBS (pH 6 and 7.4) collected after a period of 24 h of incubation were analyzed using LCMS method. LCMS spectra of OA-C=N-NH-(PEG)₂ sample incubated in PBS (pH 6) indicated the presence of fragment peak at 455 (M + 1), corresponding to the molecular weight of compound-v (Mol. Wt. = 454) (Fig. 3B). On the other hand, LCMS spectra of OA-C=N-NH-(PEG)₂ sample incubated in PBS (pH 7.4) did not show any fragment peak at 455 (Fig. 3A).

The polymer sample at acidic pH showed the presence of mass peak at 455, which indicates the hydrolytic cleavable ability of hydrazone linkage of OA-C=N-NH-(PEG)₂ polymer at acidic conditions, whereas the absence of mass peak at 455 of polymer sample incubated in PBS (pH 7.4), indicates stability of hydrazone linkage at neutral physiological pH. These results therefore indicate the suitability of OA-C=N-NH-(PEG)₂ polymer for pH-responsive delivery of VCM to the bacterial infection sites.

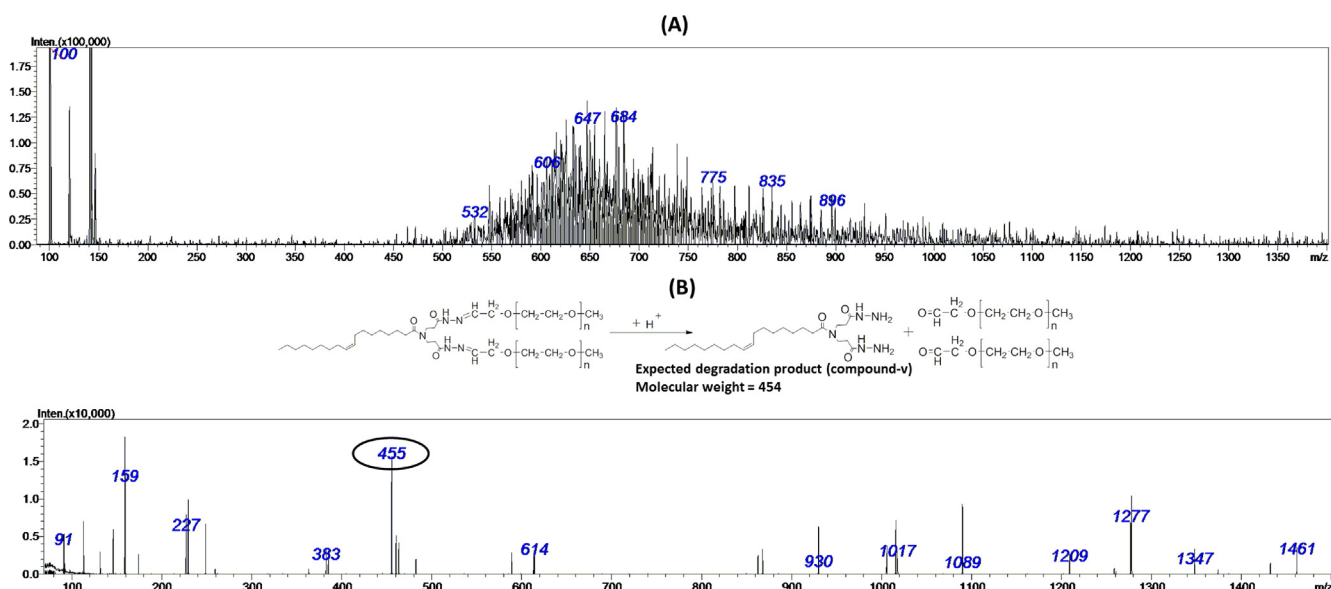


Fig. 3. LCMS spectra of OA-C=N-NH-(PEG)₂ polymer samples incubated in PBS of pH 7.4 (A) and 6 (B).

3.4. *In vitro* cytotoxicity study

The viability of cells upon their exposure to newly synthesized/formulated nanomaterials is essential to establish dosages that are safe and suitable for bio-applications (Sonawane et al., 2015). Biological efficacy of OA-C=N-NH-(PEG)₂ polymer was assessed using an *in vitro* cell culture system. Cytotoxicity studies were performed against A549, MCF7 and HepG2 cells using the MTT assay. The basic principle involved in the MTT assay is the biochemical reduction of MTT dye by viable cells via enzymatic dehydrogenase activity (Rambharose et al., 2015). The cell viability within the concentration range studied (20–100 µg/ml) was between 79.17 ± 12.67 – $78.81 \pm 6.65\%$ for A 549 cells, 86.71 ± 11.16 – $89.25 \pm 6.99\%$ for MCF 7 cells and 76.10 ± 9.00 – $76.27 \pm 6.304\%$ for Hep G2 cells (Fig. 4).

These results exhibited a dose independent effect of OA-C=N-NH-(PEG)₂ on cell viability, across all cell lines. The MTT assay results revealed that the synthesized polymer OA-C=N-NH-(PEG)₂ showed more

than 75% cell viability and showed acceptable toxicity against all cell lines tested, thereby suggesting that synthesized polymer OA-C=N-NH-(PEG)₂ was safe for biological application.

3.5. Preparation and characterization of OA-C=N-NH-(PEG)₂-VCM micelles

After the confirmation of micelles forming ability, pH-responsive degradation and non-toxicity of OA-C=N-NH-(PEG)₂ polymer, the study then proceeded to the preparation of OA-C=N-NH-(PEG)₂-VCM micelles. The VCM loaded micelles were formulated using emulsification technique, in which the polymer dissolved in a water immiscible organic solvent (DCM) was added into an aqueous solution (PBS, pH 7.4) containing VCM under vigorous stirring. The PBS solution (pH 7.4) was selected as an aqueous solvent for micelles preparation in order to provide long term storage stability to the pH-sensitive micelles (Fang et al., 2016).

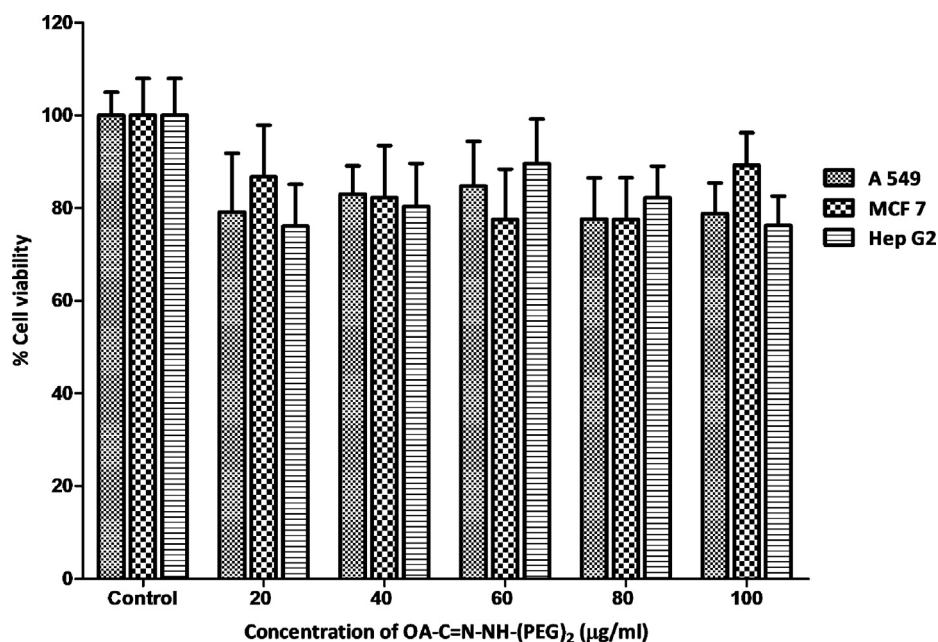


Fig. 4. Cytotoxicity assay presenting percentage cell viability after exposure of cells (A549, MCF7 and HepG2) to OA-C=N-NH-(PEG)₂ polymer (n = 6).

After overnight stirring for complete removal of DCM, micelles with particle size, PI and ZP of 130.33 ± 7.36 nm, 0.163 ± 0.009 and -4.33 ± 0.55 mV respectively were obtained. The particle size obtained for the OA-C=N-NH-(PEG)₂-VCM micelles was well below 200 nm, which is considered as ideal in order to achieve prolonged blood circulation by avoiding their scavenging by the liver and spleen (Aliabadi and Lavasanifar, 2006; Qiu et al., 2007). The size of micelles obtained in this study was in line with recently reported work, where micelles prepared using triblock copolymer containing hydrazone linkages exhibited particle size ranging from 70 to 130 nm (Qi et al., 2018). The PI of 0.163 ± 0.009 was an indication that the formulated micelles were monodisperse. The ZP plays an important role in the stability of a colloidal system. The ZP of -4.33 ± 0.55 mV indicated that micelles had a negative charge on their surfaces, which was in line with previously reported micelles formulations (Song et al., 2014; Su et al., 2016). This low ZP was due to the presence of the neutral charge on the structure of OA-C=N-NH-(PEG)₂ polymer. Although this uncharged structure of OA-C=N-NH-(PEG)₂ yielded micelles with no electrostatic repulsion, the presence of PEG chains in the micellar structure could make them sterically stable. Therefore, these parameters in general suggest that the OA-C=N-NH-(PEG)₂-VCM micelles formulated using an emulsification technique could be a superior alternative for pH-responsive delivery of VCM to the bacterial infection sites.

3.6. Surface morphology

The morphological studies using TEM showed that micelles were distinct and spherical in shape without any signs of aggregation. The size of spherical micelles obtained using TEM was in the range of 131–150 nm, which correlated well with the micelles size obtained using a zetasizer (Fig. 5A). Fig. 5B is an image captured using a blank grid to prove that the spherical shape white spots appeared in Fig. 5A were part of the grid background only and not a part of micelles. The TEM image of spherical shaped micelles therefore confirms the ability of OA-C=N-NH-(PEG)₂ polymer to assemble into a nanoformulation.

3.7. Entrapment efficiency (% EE) and drug loading capacity (LC)

The % EE and LC of VCM in the OA-C=N-NH-(PEG)₂-VCM micelles were found to be $39.61 \pm 4.01\%$ and 3.6 ± 0.36 (% w/w), respectively. % EE obtained using OA-C=N-NH-(PEG)₂ was found to be much higher, compared to previously reported amphiphilic macromolecular carriers containing hydrazone linkages, where micelles prepared using pH-responsive macromolecular carriers AM-1 and AM-2 showed % EE of 24.3 ± 0.8 and 15.8 ± 1.1 , respectively for doxorubicin (Gu et al., 2017). Micellar systems have been shown to be beneficial in enhancing the solubility and entrapment efficiency of hydrophobic drugs. The

drug loading efficiency of polymeric micelles is decided by miscibility between polymers and drugs (Xiong et al., 2011). Practically, the loading efficiency of hydrophobic drugs in polymeric micelles is mainly affected by the length of the hydrophobic block and the type of substituent present on it (Jette et al., 2004; Shuai et al., 2004). For example, modification in the core of poly(ethylene oxide)-poly(L-aspartic acid) (PEO-P (Asp)) micelles by conjugating fatty acid side chains on p (Asp), resulted in 13 times higher amphotericin B encapsulation as compared to the PEO-P(Asp) micelles containing benzyl core structures (Lavanifanar et al., 2002). Therefore, it is postulated that for OA-C=N-NH-(PEG)₂-VCM micelles, the high % EE ($39.61 \pm 4.01\%$) could be due to use of oleic acid (fatty acid) chain as a hydrophobic component in the development of amphiphilic OA-C=N-NH-(PEG)₂ polymer containing hydrazone linkage.

3.8. Dilution stability of the OA-C=N-NH-(PEG)₂-VCM micelles

Dilution stability of polymeric micelles loaded with drugs using physical methods is an important property for *in vivo* applications. This is because upon intravenous injection they are severely diluted in the bloodstream and become thermodynamically unstable, which can lead to the disaggregation of micelles and burst-release of entrapped drugs before reaching the site of action (Su et al., 2016). It has been reported in the literature that premature release of drug from polymeric micelles could significantly decrease the drug concentration at tumour sites (Deng et al., 2012; Su et al., 2016).

Therefore, to illustrate the dilution stability of OA-C=N-NH-(PEG)₂-VCM micelles, samples were diluted with PBS (pH 7.4) from 1.25 to 320-fold and changes in the particle size was measured using Zetasizer Nano ZS. It is interesting that there was no significant change observed in the sizes of OA-C=N-NH-(PEG)₂-VCM micelles up to 320-fold dilution (Fig. 6). The reason for this is that the concentration of OA-C=N-NH-(PEG)₂ polymer was $31.25 \mu\text{g/ml}$ when diluted to 320-fold, which was still above the determined CMC of the OA-C=N-NH-(PEG)₂ polymer. Therefore, these results indicate the suitability of the OA-C=N-NH-(PEG)₂-VCM micelles for *in vivo* applications due to structural integrity at high dilution values.

3.9. In vitro drug release

In vitro release profiles of bare VCM and OA-C=N-NH-(PEG)₂-VCM micelles at pH 7.4 and 6 are depicted in Fig. 7. The % drug release from bare VCM and OA-C=N-NH-(PEG)₂-VCM micelles at pH 7.4 for the initial 30 min period was 10.46 ± 2.51 and 2.13 ± 0.57 , respectively, whereas at pH 6, it was 11.10 ± 1.07 and 4.27 ± 1.61 , respectively. Afterwards, 100% release was observed for bare VCM after 8 h at pH 7.4 and 6, respectively, whereas 51.85 ± 1.54 and $57.99 \pm 3.40\%$ of VCM was released from OA-C=N-NH-(PEG)₂-VCM

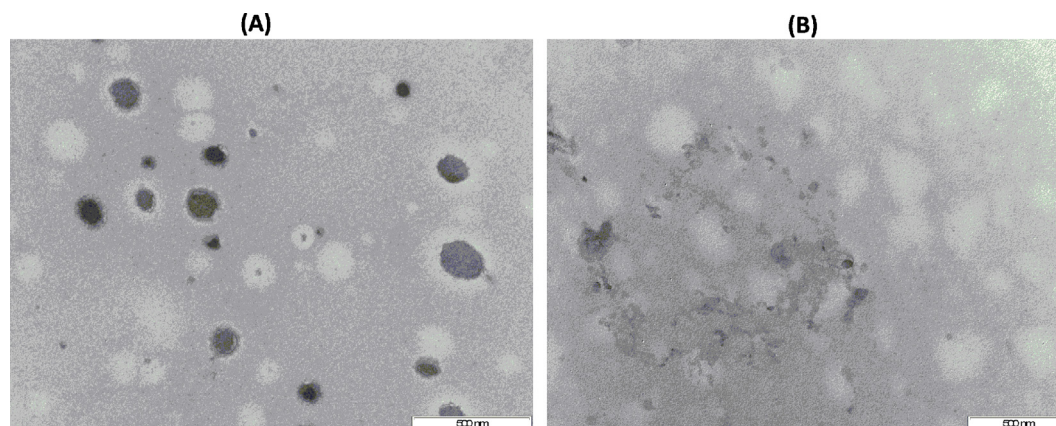


Fig. 5. Morphology of OA-C=N-NH-(PEG)₂-VCM micelles by TEM analysis (A) and TEM image showing blank grid background (B).

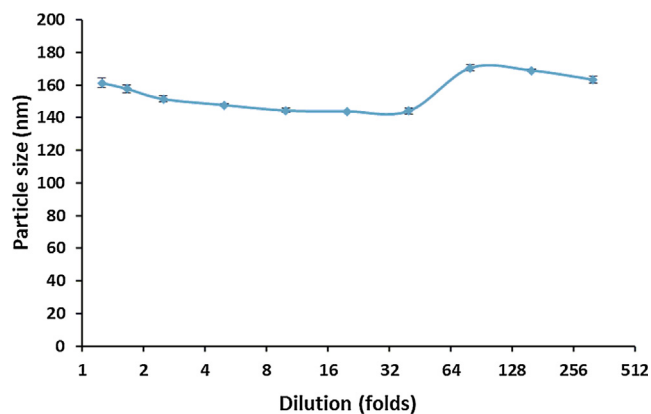


Fig. 6. Dilution stability study: size changes of OA-C=N-NH-(PEG)₂-VCM micelles against different dilutions in PBS (pH 7.4) (n = 3).

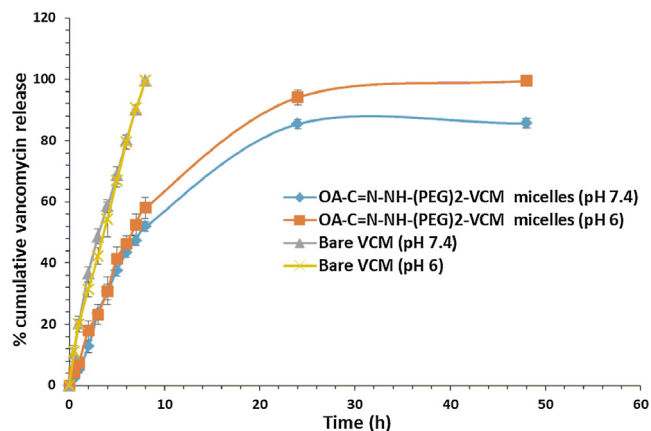


Fig. 7. *In vitro* release profiles of bare VCM and OA-C=N-NH-(PEG)₂-VCM micelles (n = 3).

micelles at pH 7.4 and 6 after 8 h, respectively. Furthermore, the release of VCM from micelles was $85.64 \pm 1.64\%$ at pH 7.4, whereas 100% VCM was released at pH 6 after 48 h incubation, respectively. As expected, the *in vitro* drug release profile of the OA-C=N-NH-(PEG)₂-VCM micelles showed faster drug release at pH 6 (corresponding to bacterial infection site), compared to pH 7.4 (neutral physiological pH). As it is well known that the lower pH of the medium enhances the hydrolysis rate of hydrazone linkages (Li et al., 2015), this faster drug release was because of the hydrolytic breakdown of hydrazone linkage of OA-C=N-NH-(PEG)₂ polymer at acidic conditions which resulted in decreased micelles stability. Therefore, the results of the *in vitro* release study confirmed stability of the formulated micelles at neutral physiological pH (pH 7.4) and their potential to release the VCM at bacterial infection site (pH 6), indicating the OA-C=N-NH-(PEG)₂-VCM micelles could be a good approach for pH-responsive delivery of antibiotics.

3.10. *In vitro* antibacterial activity

The MIC value obtained for free VCM against *S. aureus* and MRSA at pH 7.4 was 0.97 $\mu\text{g/ml}$ and 0.97 $\mu\text{g/ml}$, respectively, whereas, at pH 6 it was 1.95 $\mu\text{g/ml}$ and 0.97 $\mu\text{g/ml}$, respectively (Table 1). Blank micelles were not active against either of the bacterial strains at both pH during the entire study period, whereas VCM loaded micelles exhibited activity up to 54 h against both the bacteria. After 36 h of incubation, only OA-C=N-NH-(PEG)₂-VCM micelles showed sustained antibacterial activity, which can be attributed to the controlled release of VCM from the OA-C=N-NH-(PEG)₂-VCM micelles over 48 h (Fig. 7). At the initial time period of 18 h, the MIC value for OA-C=N-NH-(PEG)₂-VCM micelles against *S. aureus* and MRSA at pH 7.4 was 0.97 $\mu\text{g/ml}$ and

0.97 $\mu\text{g/ml}$, respectively, whereas, at pH 6 it was 0.97 $\mu\text{g/ml}$ and 0.97 $\mu\text{g/ml}$ respectively, which was similar to bare VCM against both the bacterial strains. This similar antibacterial activity of OA-C=N-NH-(PEG)₂-VCM micelles to bare VCM can be a result of quick availability of untrapped VCM from OA-C=N-NH-(PEG)₂-VCM micelles formulation to interact with bacteria after 18 h period of time (Fig. 7). After 36 h, the MIC of OA-C=N-NH-(PEG)₂-VCM micelles decreased by 2-folds against *S. aureus* at pH 7.4 and 6 respectively (MIC = 1.95 $\mu\text{g/ml}$), whereas it retained the same MIC against MRSA at both the pH values (MIC = 0.97 $\mu\text{g/ml}$) (Table 1). It is interesting to note that after 54 h, OA-C=N-NH-(PEG)₂-VCM micelles showed a 2-fold increase in antibacterial activity against *S. aureus* and MRSA at pH 6 compared to pH 7.4 (Table 1). This enhanced antibacterial activity of VCM at pH 6 can be a result of hydrolytic breakdown of the hydrazone linkage of OA-C=N-NH-(PEG)₂ polymer in acidic conditions, which led to sustained release of entrapped VCM from micelles. The lower antibacterial activity of VCM at pH 7.4 suggests the stability of hydrazone linkage at neutral physiological pH to hold the entrapped drug inside the micelle core. Therefore, the results of this study confirmed the potential of OA-C=N-NH-(PEG)₂-VCM micelles as a pH-responsive drug delivery system to enhance the performance of VCM against susceptible and resistant bacterial strains, indicating the OA-C=N-NH-(PEG)₂-VCM micelles could be used as an alternative for pH-responsive delivery of antibiotics.

3.11. *In vivo* antibacterial activity

An *in vivo* antibacterial activity of OA-C=N-NH-(PEG)₂-VCM micelles was established using a mouse skin infection model, where samples were injected intradermally into the dermis layer of the skin. Delivery of MRSA into the area between the epidermal and the subcutaneous layer was achieved by intradermal injections into the shaved skin of mice. The calculated colony-forming units (CFUs) values of each treatment group were expressed as \log_{10} (Fig. 8). It was interesting to note that, there was a statistically significant ($P = 0.0388$) depletion in bacterial concentration of the skin samples treated with OA-C=N-NH-(PEG)₂-VCM micelles, compared to the untreated control. In the OA-C=N-NH-(PEG)₂-VCM micelles treated samples, the \log_{10} CFU/ml value obtained was 3.13 ± 0.20 , which was found to be a 1.62-fold lower ($P = 0.0388$), compared to the untreated control. The \log_{10} CFU/ml value obtained for the untreated control was 5.09 ± 0.15 , which was 1.06-fold higher compared to the bare VCM treated samples (4.76 ± 0.12). These values therefore indicate that there was no statistically significant depletion ($P = 0.0566$) in the bacterial load of the skin sample treated with bare VCM after 48 h, compared to the untreated control. However, interestingly, there was a 1.52-fold reduction in MRSA load after 48 h of treatment with OA-C=N-NH-(PEG)₂-VCM micelles, compared to bare VCM ($P = 0.0260$).

The MRSA was introduced to the intradermal layer of the skin via injections with the bacteria being contained between the epidermis and subcutaneous regions. After 48 h, the presence of fluid filled abscesses were noted in the control group (Untreated). Following tissue harvesting, histomorphological analysis was performed to assess the skin integrity after the MRSA intradermal infection. Tissue sections from the untreated group showed signs of inflammation evidenced by excessive swelling of the dermal layer (Fig. 9A). The images also confirmed the formation of an abscess at the infection site, as evidenced by the abscess wall/capsule in Fig. 9A. The large area of the abscess in Fig. 9A is indicative of the extent of tissue infiltration and destruction by the 48 h MRSA infection. Due to the foreign nature of the bacteria, their introduction would have stimulated an immune response that triggered tissue inflammation and abscess formation at the infection site in an attempt to contain and destroy the invading microbes. The extent of this response is directly relative to the bacterial load in the tissue. Conversely, the OA-C=N-NH-(PEG)₂-VCM samples showed no definite signs of abscess formation although there was minimal inflammation

Table 1Sustained *in vitro* antibacterial activity results for VCM, blank micelles and VCM loaded micelles [OA-C=N-NH-(PEG)₂-VCM] (n = 3).

Formulation	MIC (µg/ml)											
	<i>S. aureus</i>						MRSA					
Bacteria												
pH	7.4			6			7.4			6		
Time (h)	18	36	54	18	36	54	18	36	54	18	36	54
Vancomycin	0.97	NA	NA	1.95	NA	NA	0.97	NA	NA	0.97	NA	NA
Blank micelles [OA-C=N-NH-(PEG) ₂]	NA	NA	NA	NA	NA	NA	NA	NA	NA	NA	NA	NA
Vancomycin loaded micelles [OA-C=N-NH-(PEG) ₂ -VCM]	0.97	1.95	3.90	0.97	1.95	1.95	0.97	0.97	1.95	0.97	0.97	0.97

NA = No activity

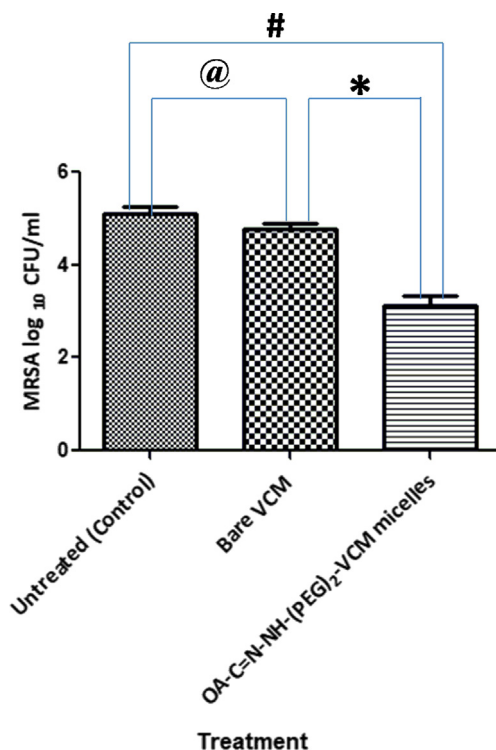


Fig. 8. MRSA load after 48 h of treatment. Data represents mean \pm SD (n = 3). # denotes significant difference when compared to untreated (control) and OA-C=N-NH-(PEG)₂-VCM micelles. @ denotes when compared to untreated (control) and bare VCM and * denotes significant difference between bare VCM and OA-C=N-NH-(PEG)₂-VCM micelles.

evident in the dermal region (Fig. 9B). Interestingly, these histological assessments are in agreement with what was observed in the *in-vivo* antibacterial study. The OA-C=N-NH-(PEG)₂-VCM samples only showed minimal signs of inflammation as it had the lowest isolated bacterial load (Fig. 8). However, the untreated control group displayed more evidence of inflammation and abscess formation as it had a statistically significant larger quantity of isolated bacteria (Fig. 8). These results provide further evidence of OA-C=N-NH-(PEG)₂-VCM micelles effectiveness as a novel nanoantibiotic for treating MRSA infections.

3.12. Stability studies

The stability studies were performed to evaluate the potential of the prepared micelles to withstand different storage conditions specified by regulatory authorities. The physical appearance, particle size, PI and ZP of the micelles stored at 4 °C and RT were evaluated to assess their storage stability. There was no change in the physical appearance including color change and aggregation of micelles throughout the storage period at 4 °C and RT for three months. The statistical analysis performed using one-way analysis of variance (ANOVA), followed by non-parametric Kruskal-Wallis and paired *t*-test showed no significant changes ($p > 0.05$) in the particle size, PI and ZP values of micelles (Table 2) stored at 4 °C. Statistical analyses performed on data obtained at RT indicated no significant changes ($p > 0.05$) in the particle size and ZP values, however there was a statistically significant change observed ($p = 0.0415$) for PI values of micelles. These results therefore confirm the storage stability of VCM loaded micelles at both 4 °C and RT.

4. Conclusion

The novel amphiphilic OA-C=N-NH-(PEG)₂ polymer containing the

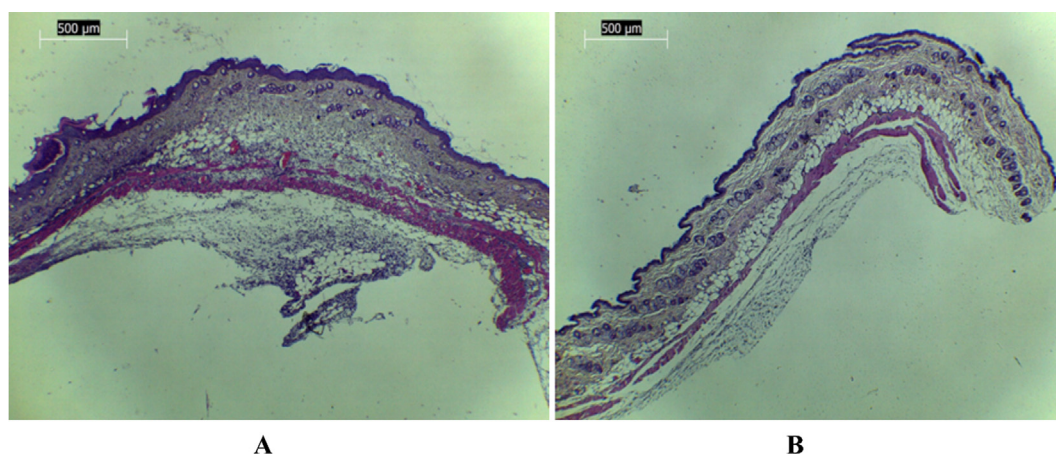


Fig. 9. Photomicrographs of the control and the treated skin selections for light microscopy (LM) stained with H&E; (X40) (A) Control (MRSA injected, untreated) (B) Treated [OA-C=N-NH-(PEG)₂-VCM].

Table 2Effect of storage condition and time on particle size, PI and ZP of VCM loaded micelles [OA-C=N-NH-(PEG)₂-VCM] (n = 3).

Storage condition	Particle size (nm)		PI		ZP	
	4 °C	RT	4 °C	RT	4 °C	RT
Time (days)						
0	130.3 ± 7.36	130.3 ± 7.36	0.163 ± 0.009	0.163 ± 0.009	-4.16 ± 0.32	-4.16 ± 0.32
30	135.6 ± 7.00	138.1 ± 8.51	0.172 ± 0.029	0.207 ± 0.011	-4.13 ± 0.53	-5.94 ± 2.38
60	137.1 ± 6.57	144.5 ± 3.04	0.169 ± 0.035	0.239 ± 0.030	-4.53 ± 0.07	-6.03 ± 0.60
90	137.2 ± 6.74	142.2 ± 3.55	0.179 ± 0.012	0.255 ± 0.048	-4.27 ± 0.27	-5.05 ± 0.35

Particle size, PI and ZP expressed as mean ± SD.

hydrazone linkage was synthesized and characterized successfully. The micelles prepared using OA-C=N-NH-(PEG)₂ polymer used to encapsulate VCM, showed pH dependent sustained drug release properties that resulted in enhanced *in vitro* antibacterial activity of VCM against *S. aureus* and MRSA at acidic pH, compared to neutral physiological pH. An anti-dilution assay performed on drug loaded micelles confirmed their circulation stability for *in vivo* antibacterial experiments. The results of *in vivo* antibacterial activity confirmed that the micelles were superior in treating resistant *S. aureus* infections as compared to bare VCM. In a field of strategic solutions to an antibiotic resistance, this biocompatible, noncomplex nano system engineered using a novel pH-responsive amphiphilic polymer would be a significant addition for the site specific delivery of VCM to treat resistant bacterial infections. In addition to antibiotic delivery, this pH-responsive micellar delivery system could be adopted for encapsulation of other classes of drugs for effective management of diseases such as cancer that are characterized by lower pH conditions.

CRediT authorship contribution statement

Sandeep J. Sonawane: Methodology, Formal analysis, Investigation, Data curation, Writing - original draft. **Rahul S. Kalhapure:** Conceptualization, Validation, Writing - review & editing, Funding acquisition. **Mahantesh Jadhav:** Project administration, Validation. **Sanjeev Rambharose:** Methodology, Investigation. **Chunderika Mocktar:** Validation, Resources. **Thirumala Govender:** Supervision, Writing - review & editing, Funding acquisition.

Declaration of Competing Interest

The authors declare that they have no known competing financial interests or personal relationships that could have appeared to influence the work reported in this paper.

Acknowledgement

The authors acknowledge the University of KwaZulu-Natal (UKZN), the National Research Foundation (NRF) of South Africa for financial support (Grant# 87790 and 88453) and South African Medical Research Council (MRC), The Biomedical Resource Unit (BRU) (UKZN) and Microscopy and Microanalysis Unit (MMU) UKZN for technical assistance, and Charlotte Ramadhin for proof reading.

References

Aliabadi, H.M., Lavasanifar, A., 2006. Polymeric micelles for drug delivery. *Expert Opin. Drug Deliv.* 3, 139–162.

Allahverdiyev, A.M., Kon, K.V., Abamor, E.S., Bagirova, M., Rafailovich, M., 2011. Coping with antibiotic resistance: combining nanoparticles with antibiotics and other antimicrobial agents. *Expert Rev. Anti Infect. Ther.* 9, 1035–1052.

Aryal, S., Hu, C.M.J., Zhang, L., 2009. Polymer-cisplatin conjugate nanoparticles for acid-responsive drug delivery. *ACS Nano* 4, 251–258.

Bae, Y., Fukushima, S., Harada, A., Kataoka, K., 2003. Design of environment-sensitive supramolecular assemblies for intracellular drug delivery: polymeric micelles that are responsive to intracellular pH change. *Angew. Chem.* 115, 4788–4791.

Bawa, P., Pillay, V., Choonara, Y.E., Du Toit, L.C., 2009. Stimuli-responsive polymers and

their applications in drug delivery. *Biomed. Mater.* 4, 1–15.

Chen, W., Meng, F., Cheng, R., Zhong, Z., 2010. pH-Sensitive degradable polymersomes for triggered release of anticancer drugs: a comparative study with micelles. *J. Control. Release* 142, 40–46.

Deng, C., Jiang, Y., Cheng, R., Meng, F., Zhong, Z., 2012. Biodegradable polymeric micelles for targeted and controlled anticancer drug delivery: promises, progress and prospects. *Nano Today* 7, 467–480.

Etrych, T., Kovář, L., Strohalm, J., Chytil, P., Říhová, B., Ulbrich, K., 2011. Biodegradable star HPMA polymer–drug conjugates: Biodegradability, distribution and anti-tumor efficacy. *J. Control. Release* 154, 241–248.

Etrych, T.S., Šírová, M., Starovoytova, L., Říhová, B., Ulbrich, K., 2010. HPMA copolymer conjugates of paclitaxel and docetaxel with pH-controlled drug release. *Mol. Pharm.* 7, 1015–1026.

Fang, X.-B., Zhang, J.-M., Xie, X., Liu, D., He, C.-W., Wan, J.-B., Chen, M.-W., 2016. pH-sensitive micelles based on acid-labile pluronic F68-curcumin conjugates for improved tumor intracellular drug delivery. *Int. J. Pharm.* 502, 28–37.

Fernandes, P., Martens, E., 2017. Antibiotics in late clinical development. *Biochem. Pharmacol.* 133, 152–163.

Ganta, S., Devalapally, H., Shahiwala, A., Amiji, M., 2008. A review of stimuli-responsive nanocarriers for drug and gene delivery. *J. Control. Release* 126, 187–204.

Gillies, E.R., Goodwin, A.P., Fréchet, J.M., 2004. Acetals as pH-sensitive linkages for drug delivery. *Bioconjugate Chem.* 15, 1254–1263.

Gu, L., Wang, N., Nusblat, L.M., Soskind, R., Roth, C.M., Uhrich, K.E., 2017. pH-responsive amphiphilic macromolecular carrier for doxorubicin delivery. *J. Bioact. Compat. Polym.* 32, 3–16.

Gupta, P., Vermani, K., Garg, S., 2002. Hydrogels: from controlled release to pH-responsive drug delivery. *Drug Discovery Today* 7, 569–579.

Jadhav, M., Kalhapure, R.S., Rambharose, S., Mocktar, C., Singh, S., Kodama, T., Govender, T., 2018. Novel lipids with three C18-fatty acid chains and an amino acid head group for pH-responsive and sustained antibiotic delivery. *Chem. Phys. Lipids* 212, 12–25.

Jette, K.K., Law, D., Schmitt, E.A., Kwon, G.S., 2004. Preparation and drug loading of poly (ethylene glycol)-block-poly (ε-caprolactone) micelles through the evaporation of a cosolvent azeotrope. *Pharm. Res.* 21, 1184–1191.

Kalhapure, R.S., Akamanchi, K.G., 2013. Oleodendrimers: A novel class of multicephalous heterolipids as chemical penetration enhancers for transdermal drug delivery. *Int. J. Pharm.* 454, 158–166.

Kalhapure, R.S., Jadhav, M., Rambharose, S., Mocktar, C., Singh, S., Renukuntla, J., Govender, T., 2017a. pH-responsive chitosan nanoparticles from a novel twin-chain anionic amphiphile for controlled and targeted delivery of vancomycin. *Colloids Surf., B* 158, 650–657.

Kalhapure, R.S., Mocktar, C., Sikwal, D.R., Sonawane, S.J., Kathiravan, M.K., Skelton, A., Govender, T., 2014. Ion pairing with linoleic acid simultaneously enhances encapsulation efficiency and antibacterial activity of vancomycin in solid lipid nanoparticles. *Colloids Surf., B* 117, 303–311.

Kalhapure, R.S., Renukuntla, J., 2018. Thermo-and pH dual responsive polymeric micelles and nanoparticles. *Chem.-Biol. Interact.* 295, 20–37.

Kalhapure, R.S., Sikwal, D.R., Rambharose, S., Mocktar, C., Singh, S., Bester, L., Oh, J.K., Renukuntla, J., Govender, T., 2017b. Enhancing targeted antibiotic therapy via pH responsive solid lipid nanoparticles from an acid cleavable lipid. *Nanomedicine* 13, 2067–2077.

Kalhapure, R.S., Suleman, N., Mocktar, C., Seedat, N., Govender, T., 2015. Nanoengineered drug delivery systems for enhancing antibiotic therapy. *J. Pharm. Sci.* 104, 872–905.

Kim, J.K., Garripelli, V.K., Jeong, U.H., Park, J.S., Repka, M.A., Jo, S., 2010. Novel pH-sensitive polyacetal-based block copolymers for controlled drug delivery. *Int. J. Pharm.* 401, 79–86.

Klevens, R.M., Edwards, J.R., Tenover, F.C., McDonald, L.C., Horan, T., Gaynes, R., System, N.N.I.S., 2006. Changes in the epidemiology of methicillin-resistant *Staphylococcus aureus* in intensive care units in US hospitals, 1992–2003. *Clin. Infect. Dis.* 42, 389–391.

Kono, K., Kojima, C., Hayashi, N., Nishisaka, E., Kiura, K., Watarai, S., Harada, A., 2008. Preparation and cytotoxic activity of poly (ethylene glycol)-modified poly (amidoamine) dendrimers bearing adriamycin. *Biomaterials* 29, 1664–1675.

Lai, T.C., Bae, Y., Yoshida, T., Kataoka, K., Kwon, G.S., 2010. pH-sensitive multi-PEGylated block copolymer as a bioresponsive pDNA delivery vector. *Pharm. Res.* 27, 2260–2273.

Lavasanifar, A., Samuel, J., Sattari, S., Kwon, G.S., 2002. Block copolymer micelles for the encapsulation and delivery of amphotericin B. *Pharm. Res.* 19, 418–422.

Lee, E.S., Na, K., Bae, Y.H., 2003. Polymeric micelle for tumor pH and folate-mediated targeting. *J. Control. Release* 91, 103–113.

- Li, H., Li, M., Chen, C., Fan, A., Kong, D., Wang, Z., Zhao, Y., 2015. On-demand combinational delivery of curcumin and doxorubicin via a pH-labile micellar nanocarrier. *Int. J. Pharm.* 495, 572–578.
- Liechty, W.B., Kryscio, D.R., Slaughter, B.V., Peppas, N.A., 2010. Polymers for drug delivery systems. *Annu. Rev. Chem. Biomol. Eng.* 1, 149–173.
- Liu, D., Yang, F., Xiong, F., Gu, N., 2016. The smart drug delivery system and its clinical potential. *Theranostics* 6, 1306–1323.
- Lu, D., Wen, X., Liang, J., Gu, Z., Zhang, X., Fan, Y., 2009. A pH-sensitive nano drug delivery system derived from pullulan/doxorubicin conjugate. *J. Biomed. Mater. Res. Part B Appl. Biomater.* 89, 177–183.
- Mhule, D., Kalhapure, R.S., Jadhav, M., Omolo, C.A., Rambharose, S., Mocktar, C., Singh, S., Waddad, A.Y., Ndesendo, V.M., Govender, T., 2018. Synthesis of an oleic acid based pH-responsive lipid and its application in nanodelivery of vancomycin. *Int. J. Pharm.* 550, 149–159.
- Pelgrift, R.Y., Friedman, A.J., 2013. Nanotechnology as a therapeutic tool to combat microbial resistance. *Adv. Drug Deliv. Rev.* 65, 1803–1815.
- Qi, P., Wu, X., Liu, L., Yu, H., Song, S., 2018. Hydrazone-containing triblock copolymeric micelles for pH-controlled drug delivery. *Front. Pharmacol.* 9, 1–11.
- Qiu, L., Zheng, C., Jin, Y., Zhu, K., 2007. Polymeric micelles as nanocarriers for drug delivery. *Expert Opin. Ther. Patents* 17, 819–830.
- Radovic-Moreno, A.F., Lu, T.K., Puscasu, V.A., Yoon, C.J., Langer, R., Farokhzad, O.C., 2012. Surface charge-switching polymeric nanoparticles for bacterial cell wall-targeted delivery of antibiotics. *ACS Nano* 6, 4279–4287.
- Rambharose, S., Kalhapure, R.S., Akamanchi, K.G., Govender, T., 2015. Novel dendritic derivatives of unsaturated fatty acids as promising transdermal permeation enhancers for tenofovir. *J. Mater. Chem. B* 3, 6662–6675.
- Rice, L.B., 2009. The clinical consequences of antimicrobial resistance. *Curr. Opin. Microbiol.* 12, 476–481.
- Sahoo, S.K., Labhasetwar, V., 2003. Nanotech approaches to drug delivery and imaging. *Drug Discov. Today* 8, 1112–1120.
- Sharma, A., Arya, D.K., Dua, M., Chhatwal, G.S., Johri, A.K., 2012. Nano-technology for targeted drug delivery to combat antibiotic resistance. *Expert Opin. Drug Deliv.* 9, 1325–1332.
- Shin, J., Shum, P., Thompson, D.H., 2003. Acid-triggered release via dePEGylation of DOPE liposomes containing acid-labile vinyl ether PEG-lipids. *J. Control. Release* 91, 187–200.
- Shuai, X., Ai, H., Nasongkla, N., Kim, S., Gao, J., 2004. Micellar carriers based on block copolymers of poly (ϵ -caprolactone) and poly (ethylene glycol) for doxorubicin delivery. *J. Control. Release* 98, 415–426.
- Sonawane, S.J., Kalhapure, R.S., Govender, T., 2017. Hydrazone linkages in pH responsive drug delivery systems. *Eur. J. Pharm. Sci.* 99, 45–65.
- Sonawane, S.J., Kalhapure, R.S., Jadhav, M., Rambharose, S., Mocktar, C., Govender, T., 2015. Transforming linoleic acid into a nanoemulsion for enhanced activity against methicillin susceptible and resistant *Staphylococcus aureus*. *RSC Adv.* 5, 90482–90492.
- Sonawane, S.J., Kalhapure, R.S., Rambharose, S., Mocktar, C., Vepuri, S.B., Soliman, M., Govender, T., 2016. Ultra-small lipid-dendrimer hybrid nanoparticles as a promising strategy for antibiotic delivery: in vitro and in silico studies. *Int. J. Pharm.* 504, 1–10.
- Song, Y., Tian, Q., Huang, Z., Fan, D., She, Z., Liu, X., Cheng, X., Yu, B., Deng, Y., 2014. Self-assembled micelles of novel amphiphilic copolymer cholesterol-coupled F68 containing cabazitaxel as a drug delivery system. *Int. J. Nanomed.* 9, 2307–2317.
- Su, Z., Liang, Y., Yao, Y., Wang, T., Zhang, N., 2016. Polymeric complex micelles based on the double-hydrazone linkage and dual drug-loading strategy for pH-sensitive docetaxel delivery. *J. Mater. Chem. B* 4, 1122–1133.
- Sugimoto, M., Morimoto, M., Sashiwa, H., Saimoto, H., Shigemasa, Y., 1998. Preparation and characterization of water-soluble chitin and chitosan derivatives. *Carbohydr. Polym.* 36, 49–59.
- Tang, R., Ji, W., Panus, D., Palumbo, R.N., Wang, C., 2011. Block copolymer micelles with acid-labile ortho ester side-chains: synthesis, characterization, and enhanced drug delivery to human glioma cells. *J. Control. Release* 151, 18–27.
- Tang, R., Ji, W., Wang, C., 2010. Amphiphilic block copolymers bearing ortho ester side-chains: pH-dependent hydrolysis and self-assembly in water. *Macromol. Biosci.* 10, 192–201.
- Topel, O., Cakir, B.A., Budama, L., Hoda, N., 2013. Determination of critical micelle concentration of polybutadiene-block-poly (ethyleneoxide) diblock copolymer by fluorescence spectroscopy and dynamic light scattering. *J. Mol. Liq.* 177, 40–43.
- Wang, X., Wu, G., Lu, C., Zhao, W., Wang, Y., Fan, Y., Gao, H., Ma, J., 2012. A novel delivery system of doxorubicin with high load and pH-responsive release from the nanoparticles of poly (α , β -aspartic acid) derivative. *Eur. J. Pharm. Sci.* 47, 256–264.
- Xiong, X.-B., Palamarzian, A., Garg, S.M., Lavasanifar, A., 2011. Engineering of amphiphilic block copolymers for polymeric micellar drug and gene delivery. *J. Control. Release* 155, 248–261.
- Xu, Z., Gu, W., Chen, L., Gao, Y., Zhang, Z., Li, Y., 2008. A smart nanoassembly consisting of acid-labile vinyl ether PEG-DOPE and protamine for gene delivery: preparation and in vitro transfection. *Biomacromolecules* 9, 3119–3126.
- Yoshida, T., Lai, T.C., Kwon, G.S., Sako, K., 2013. pH- and ion-sensitive polymers for drug delivery. *Expert Opin. Drug Deliv.* 10, 1497–1513.